Chitosan-based biomaterial and hyaluronic acid on the repair of intrabuccal bone defects in rats

Luiz Bertoldo Costa Filho,[1] Gerluza Aparecida Borges Silva,[2] Alfredo Miranda Goes,[2] Fernando Antônio Mauad de Abreu,[2] Matheus Henrique Santos Assis,[2] Alcione Soares Dutra Oliveira,[1] Fernando Oliveira Costa[2] and Peterson Antônio Dutra Oliveira[1]

[1]Pontifical Catholic University of Minas Gerais, Belo Horizonte, Brazil; [2]Federal University of Minas Gerais Gerais, Belo Horizonte, Brazil.

Abstract

Aim: This experimental study aimed to evaluate the effects of a three-dimensional matrix of chitosan-gelatin (CG) associated with 1% hyaluronic acid (HA) on gingival healing and repairing of intrabuccal bone defects in rats.

Methods: Standardized bone defects were created in the region of the upper 1st molars of rats. Study groups were created according to bone defects (n=6/group) treatment: Control group (CO); blood clot; HA group; CG group, and HA+CG group. After 7 and 21 days, the animals were sacrificed for histological and histomorphometric analysis. Bone formation was quantified as the percentage of newly synthesized collagen, visualized by Gomori's trichromic. Clinical/macroscopic evaluation was based on predetermined scores of gingival healing.

Results: Treatment with HA improved gingival healing at day 7, but no statistical differences were found among groups at day 21. The morphometric analysis demonstrated better results after the treatment of bone defects with both HA and CG at day 21. The three-dimensional structure of CG prevented the invasion of epithelial tissue into the defect, preserving its original volume.

Conclusion: Isolated use of a chitosan-gelatin osteoconductive matrix promoted greater bone deposition and preserved the volume of the surgical site, irrespective of the presence of hyaluronic acid.

Keywords: Bone repair, biomaterials, hyaluronan, chitosan-gelatin

Introduction

The replacement of bone tissue is a major challenge for dentistry, being essential for the restoration of patients' masticatory function, either by prostheses or dental implants (Morsczeck and Reichert, 2018; Spin-Neto *et al.*, 2011). Recent advances in bone tissue bioengineering have provided access to a variety of biomaterials for alveolar bone grafting and, in some cases, have allowed the early placement of dental implants (Aguilar *et al.*, 2019).

Several biomaterials have been used in the fabrication of scaffolds or three-dimensional matrices, including natural materials derived from animals or plants (collagen, starch, gelatin, alginate, cellulose, fibrin, hyaluronan, and chitosan) and synthetic materials, such as bioactive ceramics and a wide range of synthetic polymers (Aguilar *et al.*, 2019; Bhattacharyya *et al.*, 2008; Sitharaman *et al.*, 2008; Ma *et al.*, 2019; Miranda *et al.*, 2012). These materials serve as structural support (scaffold) and guides for the migration and proliferation of osteogenic cells toward the bone healing area (Abarrategi *et al.*, 2008; Bhattacharyya *et al.*, 2008; Ma *et al.*, 2019). Three-dimensional matrices of chitosan-based biomaterials (CS) have attracted the attention of researchers due to their inert nature, antibacterial properties, biodegradability, biocompatibility and low cost (Dreifke *et al.*, 2013; Miranda *et al.*, 2012). They also offer the possibility of an association with substances that promote bone formation (Oryan and Sahvieh, 2017). Adittionally, CS is easy to mould into a three-dimensional scaffold and can not only support tissue ingrowth, but also aids in the formation of tissue structure and promote growth and mineral rich matrix deposition by osteoblasts (Seol *et al.*, 2004).

Correspondence to: Fernando Oliveira Costa, Federal University of Minas Gerais. School of Dentistry, Department of Periodontology. Antonio Carlos Avenue, 6627 – Pampulha. PO Box 359 Zip Code 31270-90. Belo Horizonte, MG – Brazil. E-mail: focperio@uol.com.br

Some *in vivo* studies have shown the proliferation and adhesion of osteogenic cells to porous chitosan matrices associated with gelatin (chitosan-gelatin) during the repair of dental sockets in rats (Miranda *et al*., 2011; Miranda *et al*., 2012).

Recently, studies demonstrated the osteoinductive potential of 1% hyaluronic acid (HA) in the regenerative process of dental sockets in rats and suggested its use as a therapeutic adjuvant in dentistry (Casale *et al*., 2016; Babo *et al*., 2018). Hyaluronic acid (HA), also called sodium hyaluronate or Hyaluronan, is a component of the extracellular matrix and plays important roles in morphogenesis and tissue healing (Alcântara *et al*., 2018). It is thought to stimulate cell migration, adhesion, proliferation and differentiation that leads to bone formation. Treatment of extraction sockets with HA in rats accelerated bone deposition, confirmed by the increased expression of osteogenic proteins such as osteopontin (OPN) and bone morphogenetic protein type 2 (BMP-2) (Casale *et al*., 2016; Babo *et al*., 2018).

Although the tooth socket model in rats has been recognized as a viable model for the analysis of bone reconstruction (Miranda *et al*., 2012; Babo *et al*., 2018), cavities in this model are very small and do not represent the actual demand in terms of bone loss in clinical dentistry. For ethical, logistical, and also financial reasons, larger and standardized bone defects are more often simulated in small animals. It is worth noting that studies with chitosan-gelatin and 1% hyaluronic acid gel in intrabuccal bone defects in rats have not been reported in the literature. Individually, CS and HA have demonstrated positive results in preliminary studies *in vivo*. However, this has not been the case for CS and HA used in the combination for the treatment of bone defects where the cavity dimension and the volume of biomaterial are larger/broader and standardized.

In this sense, we hypothesized a possible synergistic effect of an osteoinductive molecule (HA) together with a scaffold (CS) that has proved to be successful in the proliferation of osteogenic cells in vitro and in vivo. Thus, the present study aimed to evaluate the effects of a tridimensional matrix graft of chitosan-gelatin, associated or not with a 1% hyaluronic acid gel, on the repair of intrabuccal bone defects in a rat model.

Materials and methods

Experimental model

In this experimental study, twenty-four 10-week-old male Wistar rats, *Rattus norvegicus albinus* were used, weighing between 300 and 350g, These animals were housed in temperature-controlled rooms and received water and food *ad libitum*. They were cared for according to the guidelines of the local Ethical Committee for Animal Research from de Federal University of Minas Gerais, had it approved the study project prior to the beginning of the experiments (protocol #2842010). When applicable, this study followed the ARRIVE (Animal Research: Reporting *in Vivo* Experiments) checklist guidelines.

Biomaterials

Hyaluronic acid ($(C_{14}H_{20}NNaO_{11})$n.Na.pH 6,2/NIKKOL was obtained from Galena, Campinas, Brazil. Three-dimensional chitosan-gelatin (CG) scaffolds were obtained by means of a freeze-drying technique and glutaraldehyde (Sigma, St. Louis, USA) cross-linking. The CG scaffolds were synthesized according to Miranda *et al.* (2011) in the Institute of Biological Sciences of the Federal University of Minas Gerais, Brazil, from two natural polymers: chitosan (Sigma, St. Louis, USA) with a degree of deacetylation of 85%, and type A porcine skin gelatin (Vetec, Rio de Janeiro, Brazil). In summary, a chitosan 0.7% (w/v) solution and a gelatin 0.7% (w/v) solution were dissolved separately in 0.1 M acetic acid. These two distinct solutions rested for 24 h at room temperature, and they were then mixed at a 3:1 (chitosan/gelatin) ratio. Subsequently, the chitosan-gelatin blend was cross-linked to a 25% glutaraldehyde solution at a 0.1% concentration. Dimensional information on the porosity patterns and the chemical and morphological aspects of the scaffolds was previously presented by Miranda *et al.* (2011), and biocompatibility, biopermeability and proper degradation of chitosan demonstrated in previous experimental studies (Sitharaman *et al*., 2008; Hou *et al*., 2012).

Surgical procedures

Rats were anaesthetized intramuscularly with a mixture of 10% ketamine (Dopalen®; Vetbrands, São Paulo, Brazil) and 2% xylazine (Ronpum®; Bayer, São Paulo, Brazil), 1:1, 0.1 mL/100g body weight, i.m. Prior to surgery, the animals received a dose of veterinary anti-inflammatory, flunixin-meglumine (Banamine® injectable PET, Cruzeiro, Brazil.), 1.1 mg/kg. The rats were then subjected to the extraction of the upper first molars (right and left). A circular defect of 2.5 mm in diameter and 2.5 mm in depth was made near the alveoli of the 1st maxillary molar using a sterile cylindrical #2094 diamond bur (KG Sorensen ISO, Brazil). The defects were created at a low rpm under copious irrigation with sterile saline. Control of bleeding and secretions was performed by vacuum aspiration. In all surgical phases, the use of cotton or gauze was avoided, as they could leave residues in the surgical site. The coaptation of the edges of the mucosa after grafting is of fundamental importance. Mattress silk sutures 6.0 (Ethicon, Jonhson & Jonhson, São Paulo, Brazil) were employed. Suture loss prior to day 7 was considered an exclusion criterion

of the samples. Bone defects (n=6 per group) were treated according to prescribed conditions for each of the four groups: 1) HA group: 30µl of 1% HA; 2) CG group: CG/chitosan-gelatin disks (1.5mm thickness x 2.5mm diameter); 3) HA+CG group: association of HA+CG; 4) CO group: defect filled with blood clot (control). An amalgam carrier was used to place the chitosan disks into the bone cavities. The sequence of the surgical procedures, details of the location and size of the bone defects are shown in figures 1 and 2.

The rats were sacrificed at 7 or 21 days after surgical procedures. In the postoperative period, the animals were kept isolated in plastic cages with access to water *ad libitum* and pasty food for 5 days. Lining the cages with wood shavings was avoided.Additionally, the rats received three subcutaneous doses (10mg/kg) of the antibiotic oxytetracycline (Terramicina® Injectable Solution; Pfizer, São Paulo, Brazil) every 24 hours.

Clinical evaluations

The effect of biomaterials on the wound healing was assessed via macroscopic photos analysis of the surgical site. Gingival healing was assessed by three trained and calibrated examiners, according to previously defined scores: 1 – maximum of 1/3 of healing wound: most of the operated area is occupied by granulation tissue; 2 – gingival epitelialization in a maximum 2/3 of the operated area; 3 – epithelialization over 2/3; 4 – complete epithelialization**.** For the definition of these scores, a preliminary study was conducted to obtain images of the maximum and minimum wound healing levels. Inter and intra-examiner agreement was assessed by weighted Kappa coefficients and showed values > 0.94.

To obtain the images, the rats were anesthetized with half a dose of anesthetic, therefore allowing animals to be immobilized and their mouth to be opened, with the aid of intraoral retractors. Photographs were taken

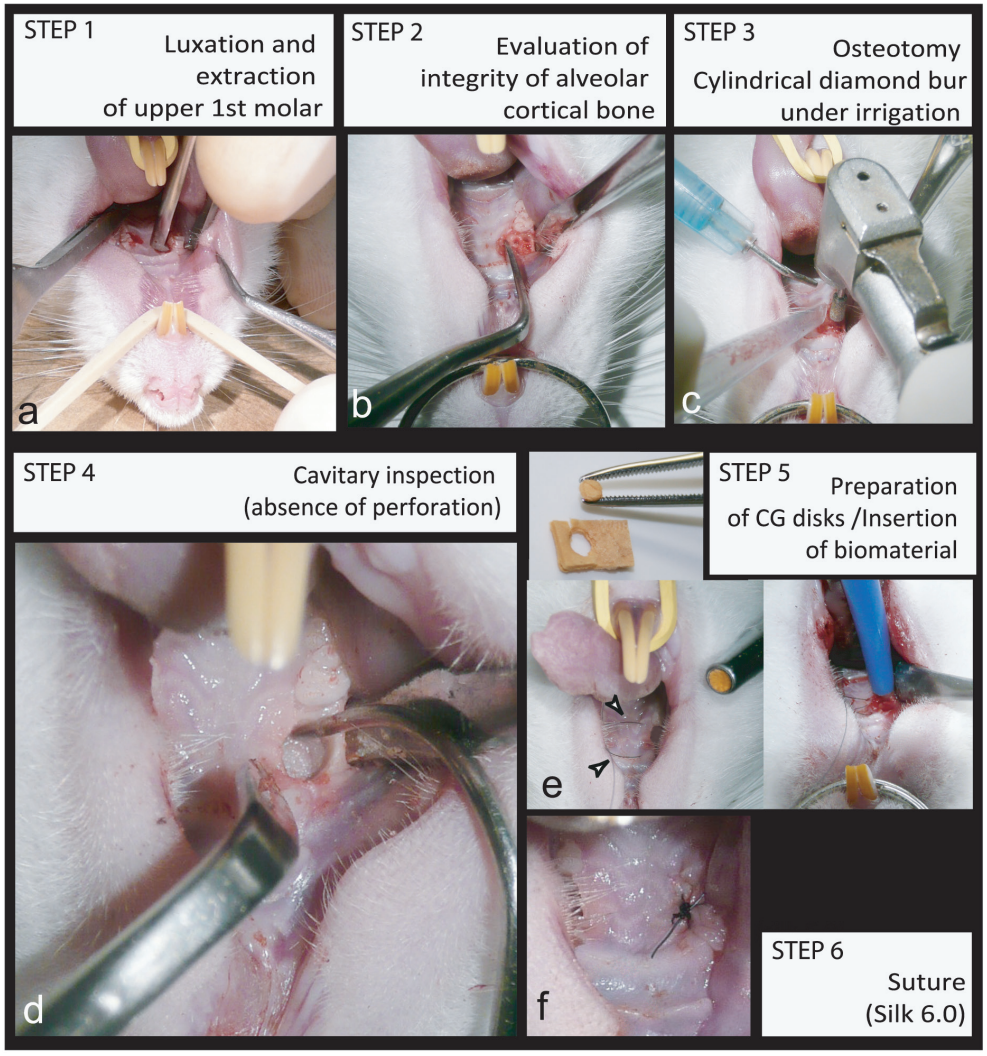

Figure 1. Surgical procedures steps. (a) Extraction of upper 1st molar; (b) Visualization of alveoli from distal roots; (c) Creation of defect with cylindrical diamond bur under irrigation and aspiration; (d) Cavitary inspection to determine the absence of perforation and the complete removal of the alveolar walls; (e) Preparation of CG disks and insertion of biomaterial; (f) Coaptation of the edges of mucosa.

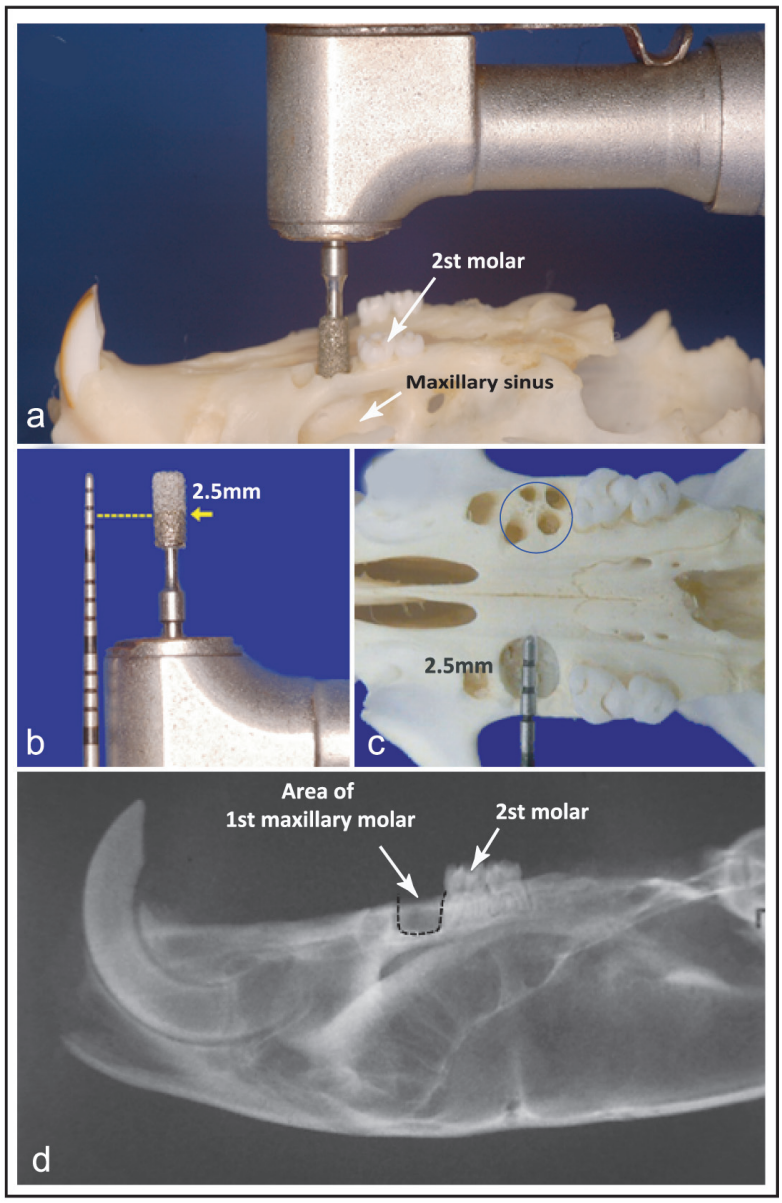

Figure 2. Location and dimensions of the bone defect in a dry skull. (a). Position of the bur perpendicular to the bone surface and parallel to the crown of the 2nd upper molar; (b). Arrow indicates the depth of the bur (2.5mm) used during the osteotomy; (c). The area circled in blue indicates the alveoli of the 4 distal roots of the upper 1st molar, which will be unified to create the defect. On the opposite side, the image illustrates the defect made with a diameter of 2.5mm; (d) Radiographic image of the defect. The radiograph was obtained with the animal in the supine position (surgical position). Dashed line indicates the limits of the bone cavity.

with a macro lens and Lumix Camera (Leika, Panasonic DMC-TZ3, New York, USA), without the use of flashes, at a standard distance of 5 cm from the object of study.

Histological procedures

After 7 and 21 days following the surgical procedures, the animals (n=24) were sacrificed by decapitation under anesthesia with 10% ketamine and 2% xylazine (1:1, 0.1 mL/100 g body weight, i.m.). Maxillae were dissected and fixed in neutral 10% buffered formalin for 72h at room temperature. After fixation, the upper maxillaries were demineralized in Planck Richol's solution, dehydrated by means of graded ethanol solutions, embedded in paraffin, and serially sectioned at 6 µm in the frontal plane. The sections were stained with Haematoxylin and Eosin (H&E) for histological analysis and Gomori's Trichrome for morphometric analysis. Four histological sections, 120 µm equidistant from one another, representing the central area of bone defect were selected from each of the 6 animals in the

same group for the quantification of bone deposition by morphometry. Images were captured with a 4x objective using the Q-color 3 camera, coupled to a light microscope (Olympus BX-41, New York, USA). Images were then transferred to a computer for morphometric analysis of bone deposition through the morphometric software ImageJ (open software, Laboratory for Optical and Computational Instrumentation, University of Wisconsin-Madison, Madison, WI, USA). This software enabled an accurate reading of percentage of collagen on the osteid and new bone trabeculae, stained in green by Gomori's trichrome (kit Leica Biosystems, Buffalo Grove, IL, US). To do so, the largest area of the defects central region was selected for measuring the green coverage percentage, which is an indicative of newly deposited bone.

Statistical analysis

Given the normality and homoscedasticity assumptions (Liliefors and Bartlett tests, respectively), data were subjected to the one-way ANOVA test, followed by the Bonferroni multiple comparison test. All analyses were performed using statistical software (Statistical Package for Social Sciences, Version for Windows – SPSS Inc., Chicago, IL, USA). Differences between groups were considered significant if a probability of < 5% significance were attained ($p<0.05$).

Results

Clinical macroscopic evaluation

The macroscopic appearance of the healing wounds was assessed at days 7 and 21. Epithelialization was incomplete at day 7 for all groups (scores 1 and 2). However, hyaluronic acid (HA) was effective as an adjuvant in the initial phase of healing (7 days) when compared to control (CO - blood clot) and chitosan-gelatin groups (CG and HA+CG). The presence of chitosan into the bone defects did not affect gingival healing, being similar to the closing of the control group at day 7 (Figure 3a). On day 21, there were no statistical differences between groups. All treatment had scores between 3 and 4, similar to the control group (Figure 3b).

Histomorphometric evaluation

Histologically, on day 7, the defects were filled with clot and fibrin network in all groups (Figure 4). An evident aspect was the process of resorption of the remaining cavity walls, apparently more accelerated in the CO and HA groups (Figure 4a and 4b) in relation to the groups that received the chitosan scaffolds, CG (Figure 4c) and HA+CG (Figure 4d) groups. In accordance with the macroscopic data, epithelial tissue was still interrupted (open) in both CO and HA groups and in the CG and HA+CG groups (Figure 4e and 4f). In CG and HA+CG groups, it was also possible to observe residues of the biomaterial (chitosan-gelatin) stained in red by the Gomori's trichrome, as shown in figures 4c and 4d respectively. At day 7, the bone deposition was minimal in all groups, histologically detected as isolated points of collagen in the apical third of the defects.

At day 21 (Figure 5), the epithelial tissue was continuous (score 4) or in the final stages of healing (score 3) in most of the samples in all groups. An interesting finding was that the three-dimensional structure of the chitosan-scaffold, present in the CG and HA+CG groups (Figures 5b and 5d), appeared to contain epithelial migration towards the interior of the bone defect, as opposed to the CO and HA groups (Figure 5a and 5c). In some cases, volume filling by chitosan-gelatin scaffolds could be clinically observed by the outline of mucosa covering the surgical site (Figre 5e).

Bone deposition in defects without CG-scaffolds (CO and HA groups) were concentrated in the deepest part (~50% of the apical area) of the defect, as observed in figures 5a and 5c. In groups with CG-scaffolds (CG and HA+CG), the area of new bone formation was more extensive.

In these groups, areas of new collagen deposition (osteoid) filled most of the defect closely associated with the chitosan laminae, suggesting the continuity of the repair process in the ~50% of the cervical cavity (Figures 5b and 5d). Figures 6e and 6f show, in the enlarged images, the presence of green-colored collagen between the chitosan sheets (red) in both CG and HA+CG groups. The histological evaluation at day 21 also showed differences in the level of bone maturation.

Defects treated with HA revealed more mature, thick and well delineated trabeculae compared to the CO group (Figure 6). The medullary spaces in the HA groups (figure 6b) were smaller suggesting a final phase of the repairing process. The CG and HA+CG groups showed bone trabeculae with more immature aspects involving wide medullary spaces (Figures 6c and 6d). In both cases, rests of the biomaterial were observed on ~50% of the superficial area of the defect underlying the oral mucosa in close contact with loose connective tissue. However, there were no signs of inflammation or fibrous tissue encapsulation of the chitosan scaffold. Pores of the scaffold were invaded by native cells of connective tissue (Figure 6g), suggesting a chemotaxis and osteoconductive action induced by the biomaterial. Areas of neovascularization, revealed by the presence of blood cells in small capillaries, were seen in close contact with the residual chitosan laminae in CG and HA+CG groups (Figure 6g). At day 21, some resorptive multinucleated cells were observed close to chitosan laminae in CG and HA+CG groups (Figure 6h), indicating the degradation mode of the biomaterial. The amount of chitosan observed in the HA+CG group was apparently lower, suggesting a faster degradation of the biomaterial when combined with HA.

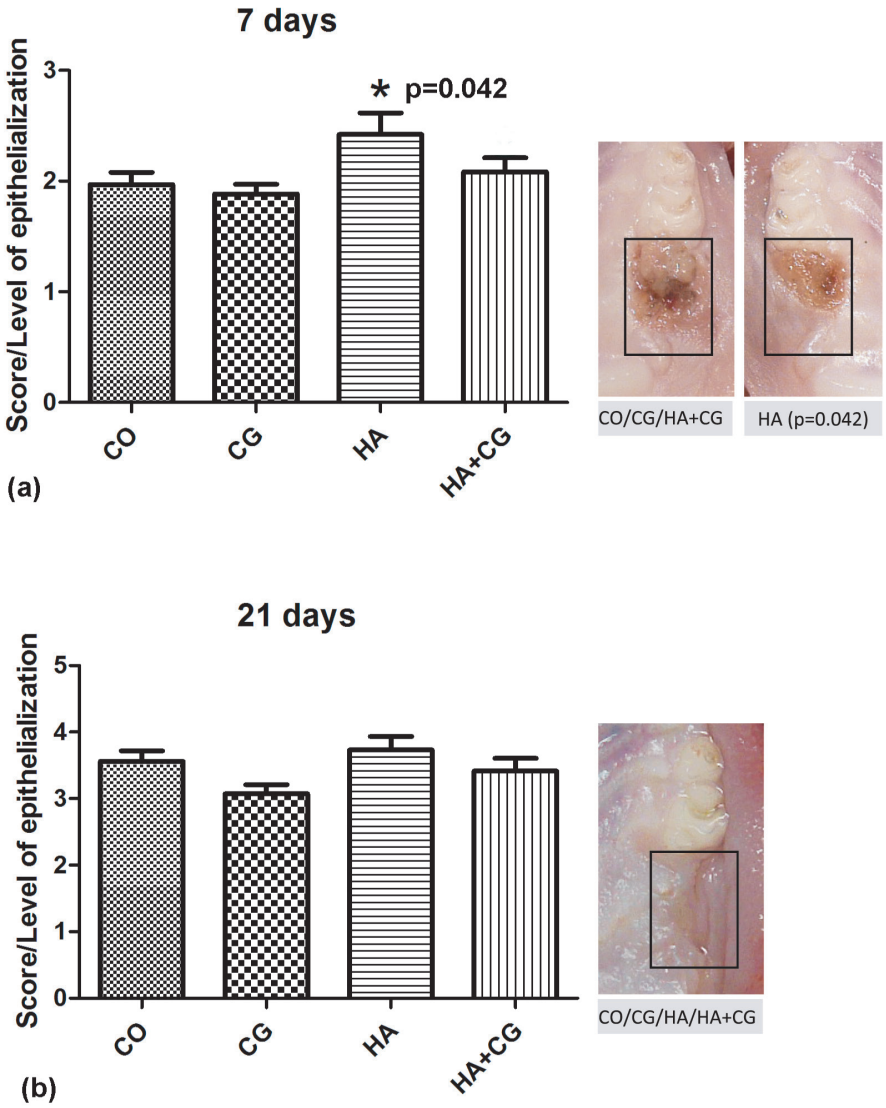

Figure 3. Comparison among mean gingival healing scores. (a) Wound healing at day 7. Treatment with HA improved gingival epithelization [HA>CO = CG= (HA+CG)]; (b) Wound healing at day 21 without statistical differences [HA= CO =CG = (HA+CG)]. Data are shown as mean±S.E.M. *Statistical difference, One-way ANOVA, followed by the Bonferroni multiple comparison test. Photographs show the macroscopic aspect of the epithelial sealing of the defect in each group

Quantification of new bone formation evaluated from collagen deposition (a) at 7 days and (b) at 21 days after surgical procedures is show in figure 7. Although the HA+CG group showed a statistically greater collagen deposition in this period, it did not exceed the limit of 1% of new bone formation (Figure 7). At day 7, bone deposition was minimal in all groups (Figure 7). The percentage of collagen increased after treatment with HA+CG for 7 days [(HA+CG) > (CO=CG) > HA]. For 21 days, collagen deposition was higher in the CG and HA groups [(HA=CG) > CO=HA+CG]. For the same space of time, the quantitative analysis revealed superior results for the bone defects treated with HA or CG (Figure 7).

Discussion

This present study demonstrated the effects of chitosan-gelatin (CG) and hyaluronic acid (HA) on the healing of intrabuccal bone defects created in rat maxillas. A novel bone defect model was utilized, which has not been published previously. This model can be considered feasible, reproducible, and appropriate for studies on bone grafting in dentistry. However, all of the pre- and post-operative care presented in the methodology of this study must be strictly followed to ensure the success of the technique.

In relation to studies of intrabuccal bone repair in rats, previous literature reported that the tooth socket model is a viable model for the analysis of bone reconstruction (Miranda *et al*., 2011; Babo *et al*., 2013). However, some

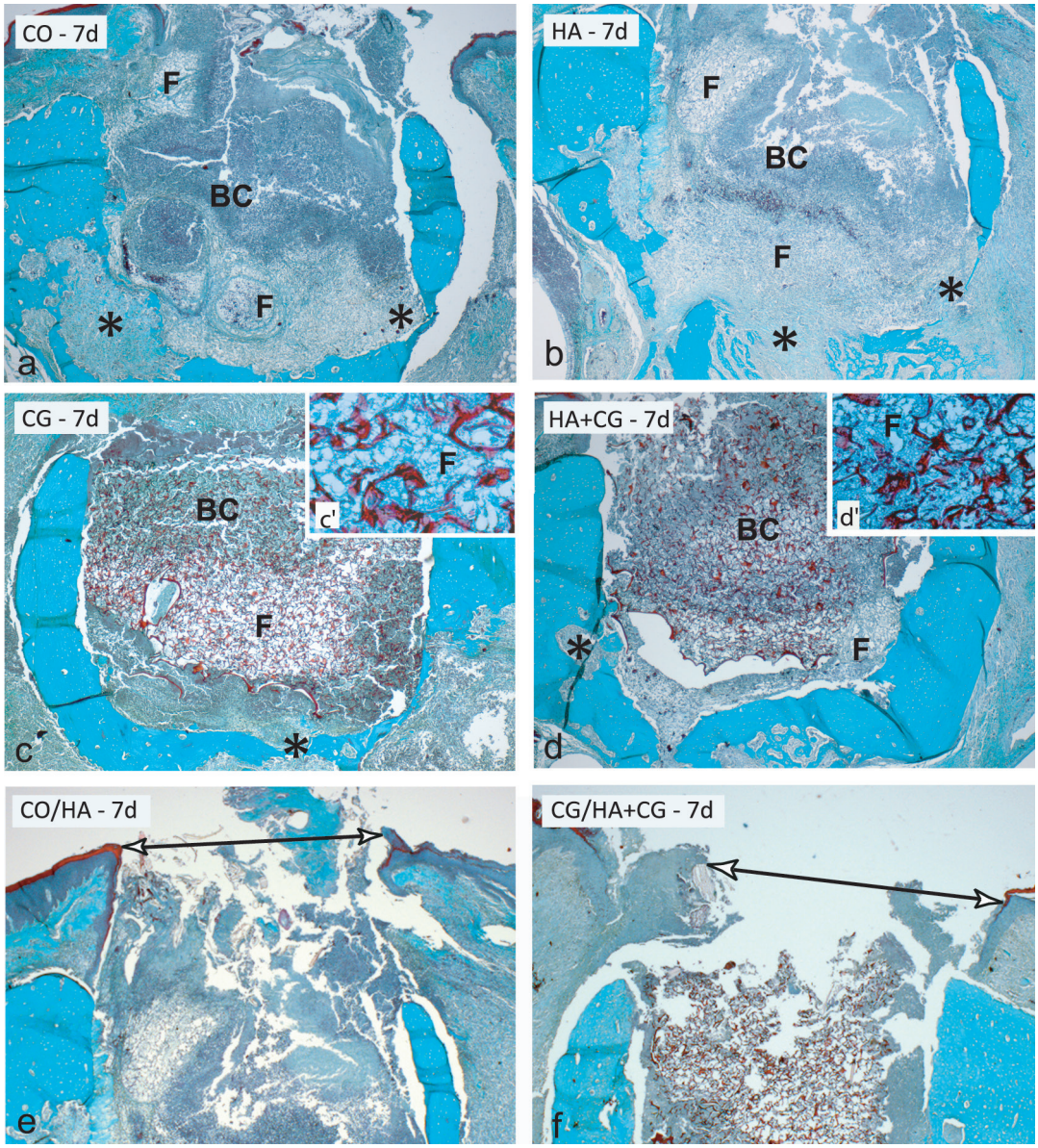

Figure 4. Histological aspect of bone repair at day 7 after surgical procedures. (a) CO group; (b) HA Group. In both CO and HA groups, the defects were filled with blood clot [BC] and fibrin network [F] without bone deposition. (c) CG group (d) HA+CG group. Layers of biomaterial shown in red with fibrin clot inside pores of chitosan (detail in c′ and d′). (e-f) Representative images of gingival healing in CO/HA, CG and HA+CG groups. At day 7, epithelium was discontinued in all groups (double arrows). (*) Areas of bone resorption were commonly found in all groups at day 7. Gomori's Trichrome. Original magnification: 4x.

technical issues must be considered for this model: the variation in the size of tooth roots and the presence of interradicular septum can hinder the insertion of solid materials, making it impossible to standardize the amount of biomaterial inserted within the bone cavities. Furthermore, intact alveoli are subject to variations in the amount of remaining periodontal ligament. This may interfere with the evolution of the inflammatory process due to the availability of osteogenic cells, thus masking the interpretation of the results (Miranda *et al.*, 2012). Larger and more standardized bone defects have been traditionally created outside of the oral cavity, such as in the tibia, femur, and calvaria of mice and rabbits (Lee *et al.*, 2010; Puricelli *et al.*, 2010; Wang *et al.*, 2017; Taz *et al.*, 2018). These sites, however, are free of factors such as bacteria, salivary flow, changes in pH and chewing forces, which prevent the direct extrapolation of results to clinical dentistry. Bone defect models more directly related to dental clinics, had it been developed in dogs and primates (Sugawara *et al.*, 2010; De Santis *et al.*, 2012; Jin *et al.*, 2014; Wang *et al.*, 2020). These experimental models are adequate as they facilitate intraoral surgical access due to its large visual field, allowing direct surgical access and the use of technical resources similar to those available at dental clinics (Elsalanty *et al.*, 2009; Baroni *et al.*, 2011; Li *et al.*, 2018). Nevertheless, the use of these animals raises issues related to ethics, costs, logistics and the need of specific vivarium.

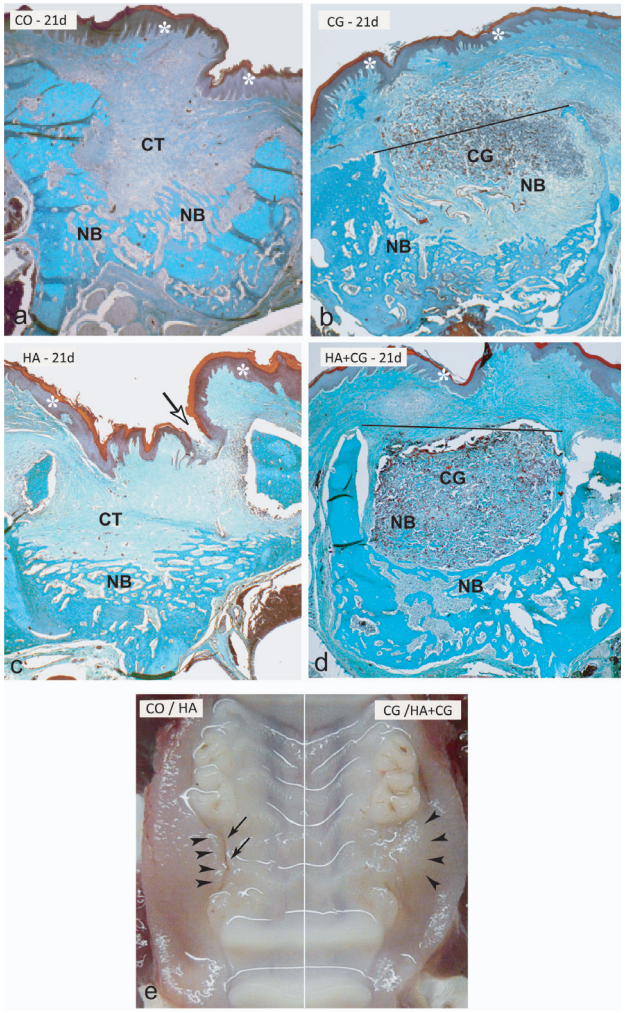

Figure 5. Histological (a-d) and macroscopical (e) images of epithelial healing after 21 days of surgical procedures. New bone deposition (NB) was concentrated in the deepest area of the defect in both the CO (a) and HA (c) groups. In these groups, ~50% of the cervical area of the defect is filled with connective tissue (CT). In the CG (b) and HA+CG (d) groups, chitosan (CG) in red occupied the largest area of the defect intercalated with newly deposited collagen matrix (green). (*) indicates the epithelium over the closed surgical site in all groups. The straight line in (b) and (d) indicates the level of the defect by the scaffold occupied by the biomaterial (CG) containing the epithelial invasion toward the interior of the bone defect. Hyaluronic acid (HA group) promotes bone deposition, but the absence of the scaffold can allow epithelial folding (arrow) into the defect. The aspect of the epithelialized mucosa over the surgical site (e) is indicated by the arrow heads in the HA (left) and CG (right) groups. Note the concave contour of the mucosa and groove (black arrow) in the epithelium, a common aspect found in the CO and HA groups suggesting epithelial invasion in the area of the surgical site that did not receive three-dimensional support of chitosan. On the opposite side (right) the mucosa is smooth and volume is apparently preserved. (a-d): Gomori's Trichrome. Original magnification: 4x.

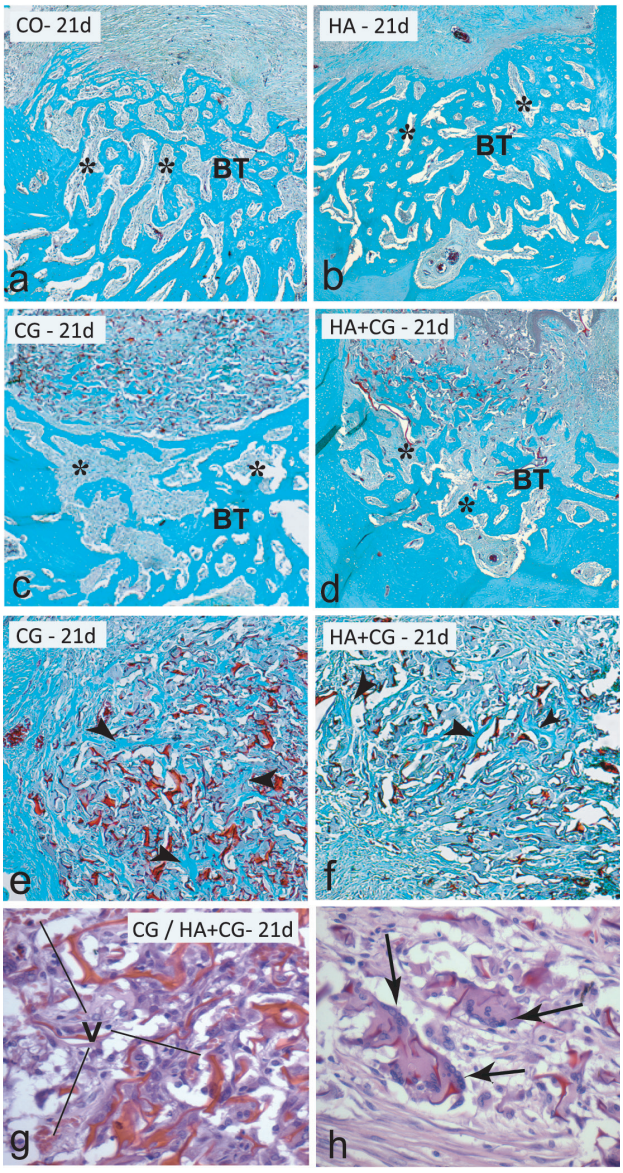

Figure 6. Histological aspect of bone repair at day 21. Note thicker bone trabeculae (BT) and smaller marrow spaces (asterisk) in the HA group (b) when compared with the CO group (a). In the CG (c) and HA+CG (d) groups, the trabeculae are more widely spaced and have larger medullary spaces, indicating a lower level of bone organization and maturation. Collagen deposition (arrows head) between residual sheets of chitosan (red) can be seen in both CG (e) and HA+CG groups (f). Image in H&E (g) shows the integration of chitosan-scaffold, observed in both groups CG and HA+CG, with native cells and vessels (V) of connective tissue. (h) Resorption of residual chitosan-gelatin (CG) scaffold by multinucleated giant cells (arrows). (a-d) Gomori's Trichrome. Original magnification: 4x. (e-f) Gomori's Trichrome. Original magnification: 10x. (g-h) H&E Original magnification: 40x

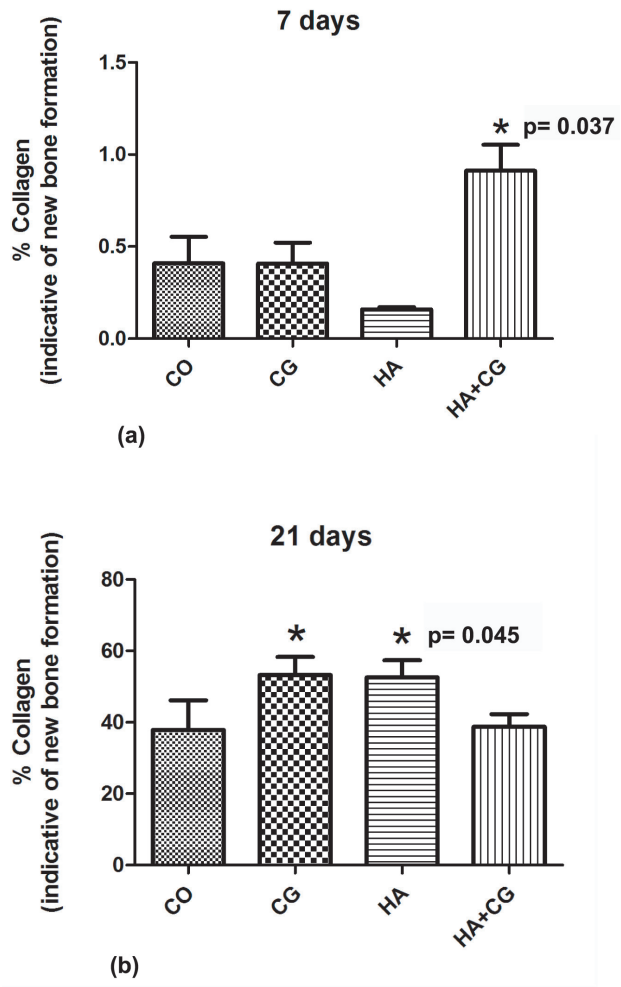

Figure 7. Quantification of new bone formation assessed from collagen deposition (a) at day 7 and (b) after 21 days of surgical procedures. Data are shown as mean±S.E.M. * # Statistical differences. One-way ANOVA, followed by the Bonferroni multiple comparison test.

In the present study, the effects of biomaterials on bone repair were evaluated at periods of 7 and 21 days. These periods were selected as the parameters in the healing process of dental sockets in rats, since at day 7 it is already possible to observe the onset of bone deposition and at day21 the alveoli are almost completely filled by newly formed bone (Babo *et al.*, 2018). Our results indicated that a period of 7 days is very brief for the evaluation of bone deposition. Morphometric data showed a minimum collagen deposition (less than 1%) during this period, even in control animals. Therefore, although statistical analysis has revealed a significantly higher percentage of collagen in the treatment with HA+CG, it is prudent to conclude that a period of 7 days is insufficient for the evaluation of this parameter. This period may be useful for evaluating other parameters that are indicatives of bone repair, such as the expression of markers of osteogenic differentiation, phenotypic characterization of initial phases of the inflammatory process, or the resorptive process preceding bone deposition. On the other hand, a 7-day period is well suited for clinical assessment and gingival healing analysis, as shown by our macroscopic evaluation. The treatment of the defects with HA has promoted a breakthrough in gingival healing observed during the first postoperative week. This finding is consistent with previous data (Yildirim *et al.*, 2018) that showed beneficial effects of HA in assisting the healing of soft tissues and acting like an anti-inflammatory agent (Bansal, *et al.*, 2010; Casale *et al.*, 2016). In dentistry, the initial closing of wounds is highly desirable in order to reduce the risk of contamination from bacteria and residuals in the oral cavity.

Although the chitosan-scaffold revealed no healing effect on the gingival tissue, its presence was not able to prevent the evolution of the healing process. At day 21, healing was almost complete and the clinical aspects in all groups were quite similar. The level of gingival healing was between scores of 3-4.

Our study demonstrated better results with isolated HA and CG. The low levels of immunogenicity and biocompatibility of the chitosan-gelatin blend, commonly cited in the literature (Huang *et al.*, 2005; Konovalova *et al.*, 2017; Oryan and Sahvieh, 2017) were confirmed by histological analyses. 7 days after implantation, the ingrowth of cells, as well as the characteristic acute inflammatory phase, could be seen even in the most central area of the scaffold. Neither necrosis of the surrounding tissues or scaffold encapsulation was observed up until 21 days, suggesting that CG was a nontoxic biocompatible matrix. These results are in agreement with Miranda *et al.* (2011) that used the same formulation of chitosan-gelatin in the evaluation of alveolar bone repair in rats. The authors used a natural and low-cost chitosan-gelatin blend scaffold, cross-linked by glutaraldehyde. Gelatin was employed as a strategy for the improvement of cell adhesion to scaffold surface, as previously described (Yang *et al.*, 2004; Lawrence and Madihally 2008). Gelatin from animal sources presents type I collagen, which is important in the formation of new bone from progenitor cells (Yang *et al.*, 2004). Gelatin is reported to improve the biological activity of chitosan, since the collagen amino acid sequences of arginine-glycine-aspartate (RGD sequence) promote cell adhesion and migration (Huang *et al.*, 2005; Lawrence and Madihally 2008).

In the histological evaluation, it was observed remaining CG-biomaterial in close contact with the connective tissue up to 21 days. Encapsulation of the biomaterial, areas of fibrosis or isolation of the biomaterial by fibrotic capsules were observed in none of the CG or HA+CG groups. It is noteworthy that the induction of fibrotic reactions around synthetic materials are not desirable properties for biomaterials (Chung *et al.*, 2017). This type of reaction that results from the activation of macrophages is one innate of the host. It can occur

with any type of biomaterial, signaling the failure of the therapy. Current studies and strategies are currently focusing on more advanced biomaterials that can modulate the innate and adaptative immune systems (Chung *et al*., 2017). In this context, chitosan presents itself as a promising biomaterial. The chitosan layers were seen in close association with several cell types, especially cells with clear nuclei and evident chromatin, a phenotype known to suggest extracellular matrix synthesis.

The adhesion and proliferation of osteoblasts on chitosan, suggested by the images of these cells and the deposition of collagen juxtaposed to the biomaterial, corroborate previous *in vitro* studies that demonstrated great advantages of chitosan in therapies for bone tissue regeneration (Aguilar *et al*., 2019).

The resorption process of chitosan-gelatin seems to be the consequence of a typical foreign body reaction that evolves into a favorable implant-tissue interaction. The chitosan-gelatin was progressively resorbed and there was a simultaneous time-compatible replacement of bone tissue, as preconized for an ideal scaffold by Donzelli *et al*. (2007). Our histological analysis showed the presence of resorptive cells in the scaffold pores in both CG and HA+CG groups. These multinucleated giant cells were more numerous and organized at day 21. Interestingly, images suggestive of a more accelerated degradation of chitosan were seen in the HA+CG group. The apparent reduction of chitosan layers observed at day 21, culminating in the reduction of the scaffold for osteogenic cells, can explain the lower deposition of collagen found in the morphometric analysis of HA+CG samples. Further studies should be conducted to evaluate the hypothesis that the presence of hyaluronic acid could accelerate the degradation of chitosan. The use of hyaluronic acid improved bone neoformation when compared to the control group, as shown by the morphometric evaluation at day 21. These results are in agreement with Babo *et al*. (2018) who observed the acceleration of bone deposition on the dental alveoli treated with HA. However, in the model developed in the present study, treatment with HA was not superior to the one with CG in relation to the percentage of collagen deposited during the same period. Both materials showed better results than the control group. However, histological assessment revealed advantages of CG compared to HA in terms of extension of the healing area and contention of epithelial invasion. Bone deposition in HA group was concentrated in the deepest area of the defect and presented outlined, thick, mature trabeculae. In the CG group, the neoformation area occupied the major part of the defect. Thus, the collagen matrix had an immature aspect, suggesting an intermediate phase of the bone repair process. This finding suggests the continuity of the process for later formation of trabeculae across the defect. In addition, the great advantage of CG over HA is the difference in the mechanical properties of these biomaterials.

It is important that biomaterials can provide a balanced ability to mechanically support initial scaffolding in the defect site, while encouraging cells to migrate into it and ignate the bone healing process (Fernandez *et al*., 2020). The micro-architecture of the gelatin-chitosan matrix is capable of supporting the oral mucosa and preventing precocious migration of the epithelial tissue into the defect, thereby preserving bone volume (Miranda *et al*., 2012). Hence, this biomaterial is also compatible with Guided Bone Regeneration (GBR) treatment (Elgai *et al*., 2017). The biological rationale underlying GBR advocates the mechanical exclusion of undesirable soft tissues from growing into the osseous defect, therefore allowing only osteogenic cell populations derived from the parent bone to repopulate the osseous wound space (Barone *et al*., 2011).

Some limitations of the present study should be pointed out such as the bone metabolism and the early healing periods in rats are significantly different from those in human bone (Danielsen *et al*., 1993). This makes it difficult to extrapolate the experimental observations to clinical conditions and this study should be regarded as a starting point for obtaining "proof of principle". Further studies aiming to validate CG as an appropriate biomaterial for GBR should be performed in other models of bone defects, considering different dimensions, topographies, as well as extending the healing evaluation to periods of 45 to 60 days, due to the current dynamics of bone repair.

Clearly, the novel model of intrabuccal bone defect of this present study creates important perspectives into biomaterials testing on the healing and/or bone regeneration in the oral cavity of low cost animal models and readily available in research laboratories. Our results demonstrated that a chitosan-gelatin blend is a biocompatible biomaterial, allowing cell adhesion and proliferation, and it is therefore desirable in the filling of bone injuries. These aspects, added to its economic viability, make chitosan-gelatin a suitable biomaterial for tissue bioengineering and a promising strategy in dentistry and regenerative medicine for bone restoration of larger defects.

Conclusion

The isolated use of a chitosan-gelatin osteoconductive matrix promoted greater bone deposition and preserved the volume of the surgical site, irrespective of the presence of hyaluronic acid (HA). Additionaly, the animal model used in the present study has a great potential use for future studies on the healing and/or bone regeneration of intrabuccal bone defects.

Source of Funding

This work was financially supported by FAPEMIG (Fundação de Amparo à Pesquisa de Minas Gerais/ Brazil) and CNPq (Conselho Nacional de Desenvolvimento Científico e Tecnológico/Brazil).

Acknowledgments and conflict of interest statement

The authors declare that there is no conflict of interest. The authors acknowledge the contribution of Dr. Igor Daniel Garcia Reis for the assistance in the treatment and care of the animals during the experiment.

References

Abarrategi A, Moreno-Vicente C, Ramos V, Aranaz I, Sanz Casado JV and López-Lacomba JL. Improvement of porous beta-TCP scaffolds with rhBMP-2 chitosan carrier film for bone tissue application. *Tissue Engineering Part A*. 2008; **14**:1305-1319.

Aguilar A, Zein N, Harmouch E, Hafdi B, Bornert F, Offner D, *et al.* Application of chitosan in bone and dental engineering. *Molecules* 2019; **19**:E3009.

Alcântara CEP, Castro MAA, Noronha MS, *et al.* Hyaluronic acid accelerates bone repair in human dental sockets: a randomized triple-blind clinical trial. *Brazilian Oral Research* 2018; **32**:e84.

Babo PS, Cai X, Plachokova AS, et al. Evaluation of a platelet lysate bilayered system for periodontal regeneration in a rat intrabony three-wall periodontal defect. *Journal of Tissue Enginnering Regenerate Medicine* 2018; **12**:e1277-e1288..

Bansal J, Kedige SD and Anand S. Hyaluronic acid: a promising mediator for periodontal regeneration. *Indian Journal of Dental Research* 2010; **21**:575-578.

Barone A, Ricci M, Calvo-Guirado JL and Covani U. Bone remodelling after regenerative procedures around implants placed in fresh extraction sockets: an experimental study in Beagle dogs. *Clinical Oral Implants Research* 2011; **22**:1131-1137.

Bhattacharyya S, Guillot S, Dabboue H, Tranchant JF and Salvetat JP. Carbon nanotubes as structural nanofibers for hyaluronic acid hydrogel scaffolds. *Biomacromolecules* 2008; **9**:505-509.

Casale M, Moffa A, Vella P, *et al.* Hyaluronic acid: Perspectives in dentistry. A systematic review. *Internantional Journal of Immunopathology and Pharmacology* 2016; **29**:572-582.

Chung L, Maestas Jr. DR, Housseau F *et al.* Key players in the immune response to biomaterial scaffolds for regenerative medicine. *Advanced Drug Delivery Reviews* 2017; **114**:184-192.

Danielsen CC, Mosekilde L and Svenstrup B. Cortical bone mass, composition, and mechanical properties in female rats in relation to age, long-term ovariectomy, and estrogen substitution. *Calcification Tissue Internantional* 1993; **52**:26-33.

De Santis E, Lang NP, Scala A, Viganò P, Salata LA and Botticelli D. Healing outcomes at implants installed in grafted sites: an experimental study in dogs. *Clinical Oral Implants Research* 2012; **23**:340-350.

Donzelli E, Salvadè A, Mimo P, Viganò M, Morrone M and Papagna R. Mesenchymal stem cells cultured on a collagen scaffold: In vitro osteogenic differentiation. *Archives of Oral Biology* 2007; **52**:64-73.

Dreifke MB, Ebraheim NA and Jayasuriya AC. Investigation of potential injectable polymeric biomaterials for bone regeneration. *Journal Biomedicine Materials Research A*. 2013; **101**:2436-2447.

Elgali I, Omar O, Dahlin C and Thomsen P. Guided bone regeneration: materials and biological mechanisms revisited. *European Journal of Oral Science* 2017; **125**:315-337.

Elsalanty ME, Zakhary I, Akeel S, *et al.* Reconstruction of canine mandibular bone defects using a bone transport reconstruction plate. *Annals of Plastic Surgery* 2009; **63**:441-448.

Fernández MP, Black C, Dawson J, Gibbs D *et al.* Exploratory full-field strain analysis of regenerated bone tissue from osteoinductive biomaterials *Materials* 2020; **13:**168**.**

Hou J , Wang J, Cao L, *et al.* Segmental bone regeneration using rhBMP-2-loaded collagen/chitosan microspheres composite scaffold in a rabbit model. *Biomedica Materials* 2012; **7**:035002.

Huang Y, Onyeri S, Siewe M, Moshfeghian A and Madihally SV. In vitro characterization of chitosan-gelatin scaffolds for tissue engineering. *Biomaterials* 2005; **26:**7616-7627.

Jin Y, Zhang W, Liu Y, *et al.* rhPDGF-BB via ERK pathway osteogenesis and adipogenesis balancing in ADSCs for critical-sized calvarial defect repair. *Tissue Engineering Part A*. 2014; **20**:3303-3313.

Konovalova MV, Markov PA, Durnev EA, Kurek DV, Popov SV and Varlamov VP. Preparation and biocompatibility evaluation of pectin and chitosan cryogels for biomedical application. *Journal of Biomedical Materials Research A*. 2017; **105**:547-556.

Lawrence BJ and Madihally SV. Cell colonization in degradable 3D porous matrices. *Cellular Adhesion & Migration* 2008; **2**:9-16.

Lee JA, Ku Y, Rhyu IC, Chung CP and Park YJ. Effects of fibrin-binding oligopeptide on osteopromotion in rabbit calvarial defects. *Journal of Periodontal & Implant Science* 2010; **40**:211-219.

Li H, Zheng J, Zhang S, Yang C, Kwon YD and Kim YJ. Experiment of GBR for repair of peri-implant alveolar defects in beagle dogs. *Science Reports* 2018; **8**:16532.

Ma Y, Xie L, Yang B and Tian W. Three-dimensional printing biotechnology for the regeneration of the tooth and tooth-supporting tissues. *Biotechnology Bioengineering* 2019; **116**:452-468.

Miranda SC, Silva GA, Hell RC, Martins MD, Alves JB and Goes AM. Three-dimensional culture of rat BMMSCs in a porous chitosan-gelatin scaffold: A promising association for bone tissue engineering in oral reconstruction. *Archives of Oral Biology* 2011; **56**:1-15.

Miranda SC, Silva GA, Mendes RM, *et al*. Mesenchymal stem cells associated with porous chitosan-gelatin scaffold: A potential strategy for alveolar bone regeneration. *Journal of Biomedical Materials Research*. Part A 2012; **100A**:2775–2786.

Morsczeck C and Reichert TE. Dental stem cells in tooth regeneration and repair in the future. *Expert Opinion Biological Therapy* 2018; **18**:187-196.

Oryan A and Sahvieh S. Effectiveness of chitosan scaffold in skin, bone and cartilage healing. *International Journal of Biological Macromollecules* 2017; **104**:1003-1011.

Puricelli E, Corsetti A, Ponzoni D, Martins GL, Leite MG and Santos LA. Characterization of bone repair in rat femur after treatment with calcium phosphate cement and autogenous bone graft. *Head & Face Medicine* 2010; **28**:6-10.

Seol YJ, Lee JY, Park YJ, *et al*. Chitosan sponges as tissue engineering scaffolds for bone formation. *Biotechnology Letters* 2004; **26**: 1037-1041.

Sitharaman B, Shi X, Walboomers XF, *et al*. In vivo biocompatibility of ultra-short single-walled carbon nanotube/biodegradable polymer nanocomposites for bone tissue engineering. *Bone* 2008; **43**:362-370.

Spin-Neto R, Marcantonio EJ, Gotfredsen E and Wenzel A. Exploring CBCT-based DICOM files. A systematic review on the properties of images used to evaluate maxillofacial bone grafts. *Journal of Digital Imaging* 2011; **24**:959-966.

Sugawara A, Fujikawa K, Hirayama S, Takagi S and Chow LC. In vivo characteristics of premixed calcium phosphate cements when implanted in subcutaneous tissues and periodontal bone defects. *Journal of Research of the National Institute of Standards and Technology* 2010; **115**: 277-290.

Taz M, Bae SH, Jung HI, Cho HD and Lee BT. Bone regeneration strategy by different sized multichanneled biphasic calcium phosphate granules: In vivo evaluation in rabbit model. *Journal of Biomaterials Applied* 2018; **32**:1406-1420.

Wang G, Roohani-Esfahani SI, Zhang W, *et al*. Effects of Sr-HT-Gahnite on osteogenesis and angiogenesis by adipose derived stem cells for critical-sized calvarial defect repair. *Science Reports* 2017; **7**:41135.

Wang S, Yang Y, Koons GL, *et al*. Tuning pore features of mineralized collagen/PCL scaffolds for cranial bone regeneration in a rat model. *Materials Science Engineering C* 2020; **106**:110186.

Yang C, Yang S, Du J, Xiao B and YE S. Biocompatibility studies on bone marrow stromal cells with chitosan-gelatin blends. *Journal of Wuhan University of Technology- Materials Science Edition* 2004; **19**:30-33.

Yıldırım S, Özener HÖ, Doğan B and Kuru B. Effect of topically applied hyaluronic acid on pain and palatal epithelial wound healing: An examiner-masked, randomized, controlled clinical trial. *Journal of Periodontology* 2018; **89**:36-45.